Volatile Methyl Siloxane Atmospheric Oxidation Mechanism from a Theoretical Perspective – How is the Siloxanol Formed?

Mitchell W. Alton[1,2,&], *Virginia L. Johnson*[1], *Sandeep Sharma*[1], *Eleanor C. Browne**[1,2]

[1] Department of Chemistry, University of Colorado, Boulder, Colorado 80309, United States

[2] Cooperative Institute for Research in Environmental Sciences, University of Colorado, Boulder, Colorado, 80309, United States

[&]Now at Aerodyne Research, Inc. Billerica, Massachusetts, 01809, United States

KEYWORDS Siloxanes, atmospheric oxidation reactions, isomerization, autoxidation, reaction rates.

ABSTRACT

Despite several investigations on the atmospheric fate of cyclic volatile methyl siloxanes (VMS), the oxidation chemistry of these purely anthropogenic, high production volume compounds is poorly understood. This has led to uncertainties in the environmental impact and fate of the

oxidation products. According to laboratory measurements, the main VMS oxidation product is the siloxanol (a -CH_3 replaced with an -OH), however, none of the mechanisms proposed to date satisfactorily explain its formation. Motivated by our previous experimental observations of VMS oxidation products, we use theoretical quantum chemical calculations to 1) explore a previously unconsidered reaction pathway to form the siloxanol from reaction of a siloxy radical with gas-phase water, 2) investigate differences in reaction rates of radical intermediates in hexamethylcyclotrisiloxane (D3) and octamethylcyclotetrasiloxane (D4) oxidation, and 3) attempt to explain the experimentally observed products. Our results suggest that while the proposed reaction of the siloxy radical with water to form the siloxanol can occur, it is too slow to compete with other unimolecular reactions and thus cannot explain the observed siloxanol formation. We also find that the reaction between the initial D3 peroxy radical ($RO_2^\bullet$) with $HO_2^\bullet$ is slower than previously anticipated (calculated as 3×10^{-13} cm^3 $molec^{-1}$ s^{-1} for D3 and 2×10^{-11} cm^3 $molec^{-1}$ s^{-1} for D4 compared to the general rate of $\sim1\times10^{-11}$ cm^3 $molec^{-1}$ s^{-1}). Finally, we compare the anticipated fates of the $RO_2^\bullet$ under a variety of conditions and find that reaction with NO (assuming a general $RO_2^\bullet$ + NO bimolecular rate constant of 9×10^{-12} cm^3 $molec^{-1}$ s^{-1}) will likely be the dominant fate in urban conditions while isomerization can be important in cleaner environments.

1 Introduction

Cyclic volatile methyl siloxanes (cVMS, or simply VMS) are high production volume chemicals[1,2] that are common components in consumer products such as personal care products and are intermediates in the production of silicone sealants and lubricants. Once these chemicals are released into the environment >90% of these compounds will partition into the atmosphere due to their high vapor pressure and low water solubility.[3] In the atmosphere, the main transformation mechanism is oxidation by $^\bullet$OH radicals (and in some locations $^\bullet$Cl atoms) leading to lifetimes of

VMS parent molecules between a couple of days for decamethylcyclopentasiloxane (D5) to longer than a week for hexamethylcyclotrisiloxane (D3)[4,5] Experimental studies suggest that the major first-generation oxidation products are the siloxanol (R_3SiOH) and/or the formate ester products ($R_3SiOCHO$),[3,4,6–8] with the siloxanol product detected previously in ambient particulate matter.[9] However, the mechanism through which these molecules are formed remains uncertain.

It is accepted that initial VMS oxidation occurs via a hydrogen abstraction from one of the methyl groups by $^{\bullet}OH$ radicals or $^{\bullet}Cl$ atoms[10–12] forming an alkyl radical that will quickly react with O_2 to form a peroxy radical ($RO_2^{\bullet}$), in this case $R_3SiCH_2O_2^{\bullet}$. $RO_2^{\bullet}$ fate depends on atmospheric conditions. Specifically, the $RO_2^{\bullet}$ can undergo bimolecular reactions with NO, $HO_2^{\bullet}$, or other $RO_2^{\bullet}$ in addition to unimolecular isomerization/autoxidation if it has a sufficiently long lifetime.[11,13–15] Investigations using electronic structure calculations have proposed pathways for the formation of the formate ester product under conditions where $R_3SiCH_2O_2^{\bullet}$ fate is dominated by reaction with NO.[11,12] However, the proposed mechanism requires two conversions of NO to NO_2 and is thus inconsistent with previous experiments that suggest only one molecule of NO is consumed during the first-generation of VMS oxidation.[16,17] Additionally, our own recent experimental work suggests that the siloxanol, rather than the formate ester, is preferentially formed in the oxidation of octamethylcyclotetrasiloxane (D4) and decamethylcyclopentasiloxane (D5). Under conditions of long $RO_2^{\bullet}$ lifetime where unimolecular isomerization can occur, computational studies suggest that all the methyl groups will be rapidly transformed to hydroxyl groups.[11] Experimental results however detect mainly the single hydroxyl siloxanol species,[4,6] though siloxanols with multiple -CH_3 to -OH conversions have been detected experimentally with lower apparent yields.[6,18]

Overall, the formation mechanism of 1-hydroxypentamethylcyclotrisiloxane and 1-hydroxyseptamethylcyclotetrasiloxane (siloxanol products of D3 and D4) as major closed-shell

oxidation products remains uncertain. Moreover, our previous experimental work suggested that the distribution of first-generation products was largely independent of $RO_2^{\bullet}$ fate for D4 and D5 in contrast to hexamethylcyclotrisiloxane (D3) for which the product distribution did change as a function of $RO_2^{\bullet}$ fate.[6] To explain the formation of the single siloxanol and the relative insensitivity of product distribution to $RO_2^{\bullet}$ fate, we proposed two hypotheses in Alton and Browne (2022).[6] For the first (H1), we proposed that the $RO_2^{\bullet}$ isomerization rate increases as a function of ring-size to the point where it can be competitive with bimolecular reactions across a range of $RO_2^{\bullet}$ lifetimes. Thus, even under relatively high NO conditions, the radical could isomerize. Following isomerization, the resulting radical decomposes producing formaldehyde and a siloxy radical. We postulated that the resulting siloxy radical ($R_3SiO^{\bullet}$) would react with gas-phase water or $HO_2^{\bullet}$ generating the siloxanol, rather than undergoing rapid unimolecular hydrogen shifts.[6] For the second hypothesis (H2), we put forth the possibility that instead of isomerization outcompeting bimolecular reactions, $RO_2^{\bullet}$ bimolecular reactions with $HO_2^{\bullet}$ preferentially form $R_3SiCH_2O^{\bullet}$ rather than the hydroperoxide product, particularly in the cases of D4 and D5 oxidation.[6] Subsequent siloxanol formation would require the existence of a currently unknown pathway starting from $R_3SiCH_2O^{\bullet}$. This second hypothesis was based on the observation that the product distribution remained largely invariant despite changes in the fate of $RO_2^{\bullet}$ and the assumption that the reaction of $R_3SiCH_2O_2^{\bullet}$ with NO will preferentially form $R_3SiCH_2O^{\bullet}$. Additionally, we observed low signal levels attributed to the hydroperoxide product. While low hydroperoxide signals could be in part explained by low sensitivity of our analytical technique to hydroperoxides, it is unlikely to be the sole reason.[6] This type of radical propagating channel of $RO_2^{\bullet}$ + $HO_2^{\bullet}$ reactions is relatively uncommon in atmospheric chemistry, but has been proposed to occur before in other systems.[19]

Here, we use electronic structure calculations and transition state theory to investigate the plausibility of these hypotheses for $R_3SiCH_2O_2^{\bullet}$ and $R_3SiO^{\bullet}$ radicals derived from both D3 and D4. This work builds off prior computational investigations of tetramethylsilane[12] and hexamethyldisiloxane (L2) and D3[11] by expanding the computations to larger VMS species, investigating the $R_3SiCH_2O_2^{\bullet}$ + $HO_2^{\bullet}$ potential energy surface, and exploring the feasibility of the bimolecular reaction of $R_3SiO^{\bullet}$ with gas-phase water.

2 Methods

We used Gaussian 16, Revision A.03[20] to perform all geometry optimization and single-point energy calculations unless otherwise stated. Calculations were completed on the Rocky Mountain Advanced Computing Consortium's Summit supercomputer.[21] Both B3LYP and M06-2X functionals have been used for optimization calculations by previous studies,[8,11,12] though M06-2X has been suggested to be more accurate.[11] A comparison of the results from the two levels of theory are presented in Section S1 of the Supporting Information. For D3 calculations we used both functionals, but due to the cost of the calculations on the larger D4 molecule, only the M06-2X functional was considered. D5 was not investigated due to its high computational costs and because in previous experimental investigations D5 showed similar product yields to D4.[6] The basis set for optimization was kept constant for both functionals at 6-31G+(d,p). Single point energy calculations at the CCSD(T)/cc-pVDZ level have shown good agreement to experimental energy for similar systems.[12] Single point energy calculations for the D4 reaction were carried out with MRCC[22] using the frozen core approximation of UCCSD(T)/cc-pVDZ.[23]

All transition state structures were confirmed to only have one imaginary frequency, and all other structures had only real frequencies. Transition states that do not involve a H-shift were confirmed to link to the starting and ending products using an internal reaction coordinate

calculation. Coordinates of all optimized transition state structures are listed in Section S2 of the Supporting Information. We explored different conformers of the $RO_2^{\bullet}$ and used the conformer with the lowest energy for subsequent calculations. A higher energy conformer was also investigated for the D4-derived $RO_2^{\bullet}$, and our main conclusions were found to be invariant. More details on the different conformer investigated are presented in Section S3 of the Supporting information.

Gibbs free energies of all structures were determined using the structural and vibrational information from DFT and the CCSD(T)/cc-pVDZ single point energies. Reported rate constants were calculated with transition state theory (TST) at the high-pressure limit; k_{TST} can be found via Equation 1:

$$k_{TST}(T) = \kappa \frac{k_B T}{h} \frac{Q_{TS}}{Q_{Reac}} e^{-\frac{\Delta E}{k_B T}} \quad (1)$$

where κ is the Wigner tunneling correction, k_B and h are the Boltzmann constant and Planck's constant, respectively, and T is the temperature in Kelvin.[24] The transition state and reactant partition functions, Q_{React} and Q_{TS}, are solved using *ab initio* values from the DFT methods outlined above. The change in energy, ΔE, is calculated from single point energies with zero-point vibrational corrections at the optimization level of theory.

Using the *ab initio* harmonic frequencies and single point energies calculated, the Gibbs free energies of the structures were determined per previously established methods.[25] All reported Gibbs free energies are calculated at 298 K. We compared our theoretical results to previously published experimental work.[6] In that work, VMS were oxidized in a 1 m^3 chamber under conditions that were expected to favor $RO_2^{\bullet}$ reactions with $HO_2^{\bullet}$, NO, or $RO_2^{\bullet}$ isomerization. In short, these results showed that the formate ester product was the most abundant product in D3 oxidation with high NO, but otherwise the siloxanol was the most abundant product. Scheme 1

shows the overall reaction mechanism of VMS oxidation as it is currently understood from a theoretical perspective, using D4 as an example VMS, with the specific reactions we proposed in this work in the dashed boxes. In this work, we are looking at specific reactions that might reconcile the experimental observations and theoretical mechanism.

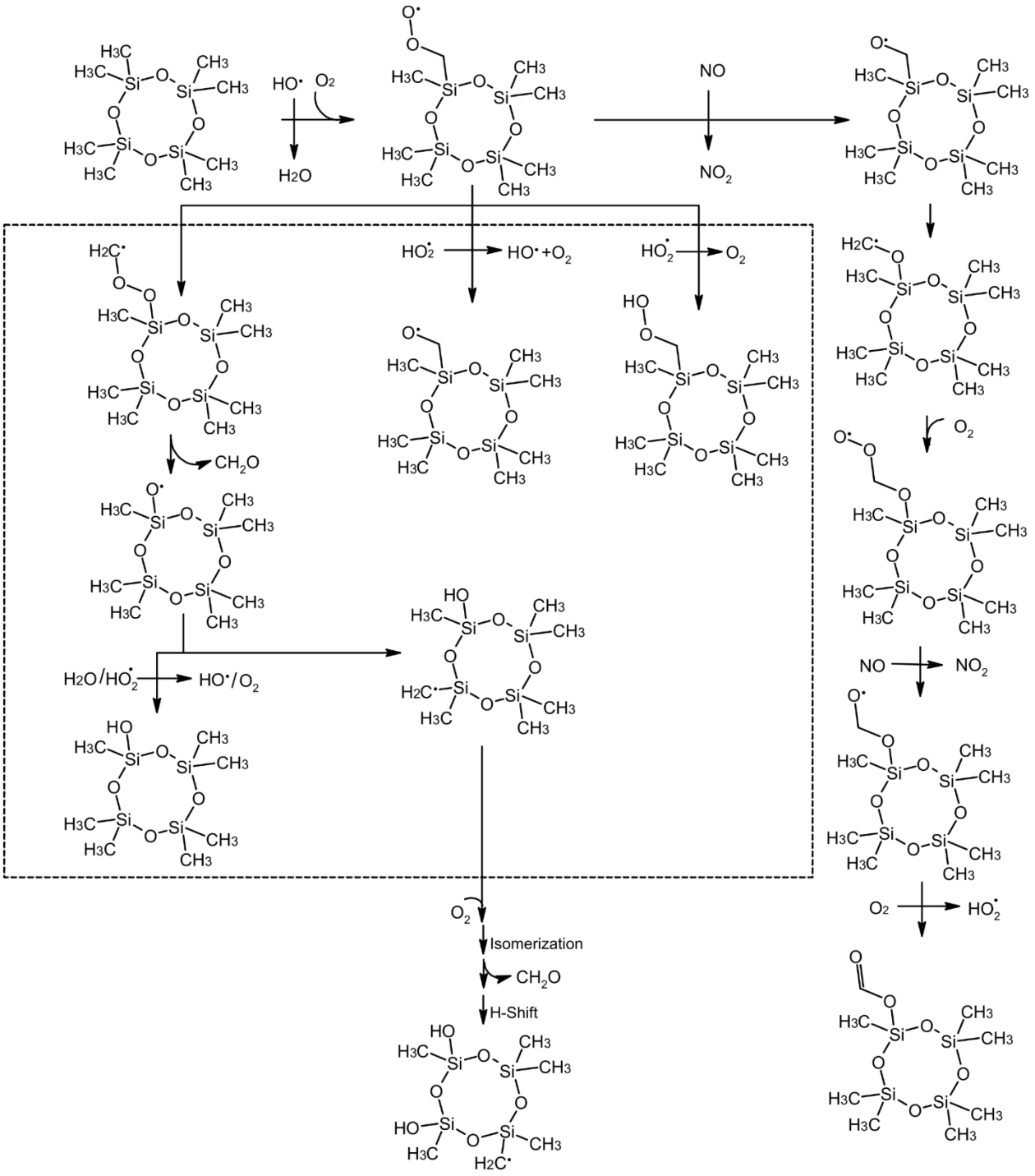

Scheme 1 Schematic for VMS oxidation mechanism as it is currently understood. Reactions in the dashed boxes are proposed reactions are investigated in this work.

3 Results and Discussion

3.1 $R_3SiCH_2O_2^{\bullet}$ isomerization and subsequent $R_3SiO^{\bullet}$ reactions

In this section we investigate the hypothesis (H1) that the $RO_2^{\bullet}$ isomerization rate increases as ring size increases and that the subsequently formed siloxy radical reacts with H_2O or $HO_2^{\bullet}$ to form the siloxanol product.

3.1.1 Unimolecular reactions of $R_3SiCH_2O_2^{\bullet}$

Figure 1 shows the potential energy surface (PES) of the different unimolecular reactions considered for D3 and D4 and Table 1 reports the energies and calculated rate coefficients for the different unimolecular $RO_2^{\bullet}$ reactions. The reaction with the lowest free energy barrier (and most likely pathway) for both D3 and D4 is an unusual rearrangement reaction ($TS_{1\text{-}5}$) of the peroxy group to form a peroxide alkyl radical with a ΔE of 19.4 kcal/mol for D3 and 21.3 kcal/mol for D4. The result for D3 is in good agreement (within 5%) with previous literature, which has reported a ΔE of 18.4 kcal/mol for D3.[11] It has been previously calculated that this peroxide alkyl radical rapidly decomposes releasing formaldehyde and forming the siloxy radical $R_3SiO^{\bullet}$.[11,12] We were unable to find a transition state for the decomposition of this peroxide alkyl radical in this work, suggesting this is a very weakly bound transition state.

Table 1 Results from theoretical calculations of $RO_2^{\bullet}$ reactions with the M06-2X functional optimized geometries.

Reaction	VMS	ΔG (kcal/mol)[a]	ΔE (kcal/mol)[b]	k (s^{-1})
$R_3SiCH_2O_2^{\bullet} \rightarrow R_3SiOCH_2O^{\bullet}$[c]	D3	46.3	42.2	4×10^{-20}
($TS_{1\text{-}1}$)	D4	44.8	42.3	1×10^{-18}
$R_3SiCH_2O_2^{\bullet} \rightarrow R_3SiC^{\bullet}HOOH$	D3	45.0	41.2	2×10^{-17}
($TS_{1\text{-}2}$)	D4	44.3	40.8	7×10^{-17}
$R_3SiCH_2O_2^{\bullet} \rightarrow {}^{\bullet}R_3SiCH_2OOH$ (1,5 Shift)	D3	33.8	28.9	1×10^{-9}
($TS_{1\text{-}3}$)	D4	33.1	29.3	8×10^{-9}
$R_3SiCH_2O_2^{\bullet} \rightarrow {}^{\bullet}R_3SiCH_2OOH$ (1,7 shift)	D3	30.7	24.6	3×10^{-7}
($TS_{1\text{-}4}$)	D4	30.7	25.4	5×10^{-7}
$R_3SiCH_2O_2^{\bullet} \rightarrow R_3SiO_2C^{\bullet}H_2$	D3	21.2	19.4	1×10^{-2}
($TS_{1\text{-}5}$)	D4	22.3	21.3	3×10^{-3}

[a]The ΔG is the Gibbs free energy difference of the reactants and the transition state structures at 298 K and is corrected for zero-point vibrational energies. [b]ΔE reported here is corrected for zero-point vibrational energies. [c]This reaction was previous proposed by Atkinson (1995)[7] to explain formate ester product.

Other pathways investigated include the reaction proceeding through $TS_{1\text{-}1}$ (colored pink in Figure 1) and hydrogen-shift reactions. The reaction proceeding through $TS_{1\text{-}1}$ was previously suggested from experimental studies as an intermediate to form the formate ester product.[7] Despite its low energy product, the large energy barrier (ΔE of 42.2 and 42.3 kcal/mol for D3 and for D4, respectively) makes this reaction unlikely, which is consistent with previous theoretical studies.[11,12] Previous literature using CBS-QB3//M06-2X/6-31+G(d,p) for their calculations has reported the energy barrier, ΔE, of $TS_{D3\_1\text{-}2}$ as 48.2 kcal/mol,[11] which higher (by ~12%) than our results. For the hydrogen-shift reactions, we explored abstraction from a methyl group on the same Si atom as the RO_2 ($TS_{1\text{-}3}$), a methyl group on a nearby Si atom ($TS_{1\text{-}4}$), and from the carbon the

peroxy group is directly bonded to (TS_{1-2}). All these H-shift reactions have relatively high energy barriers (ΔG) for both D3 and D4 (~25 to 45 kcal/mol), with the abstraction from the methyl group on an adjacent Si atom most favorable, which is consistent with previous studies on D3 and the smaller, linear, hexamethyldisiloxane.[11] We note that given the computational costs we did not investigate the H-shift reactions on D4 for the methyl group across the ring from the peroxy radical. Hydrogen abstraction reactions from various methyl groups to form a hydroperoxide and an alkyl radical are less favorable than the rearrangement reaction TS_{1-5}.

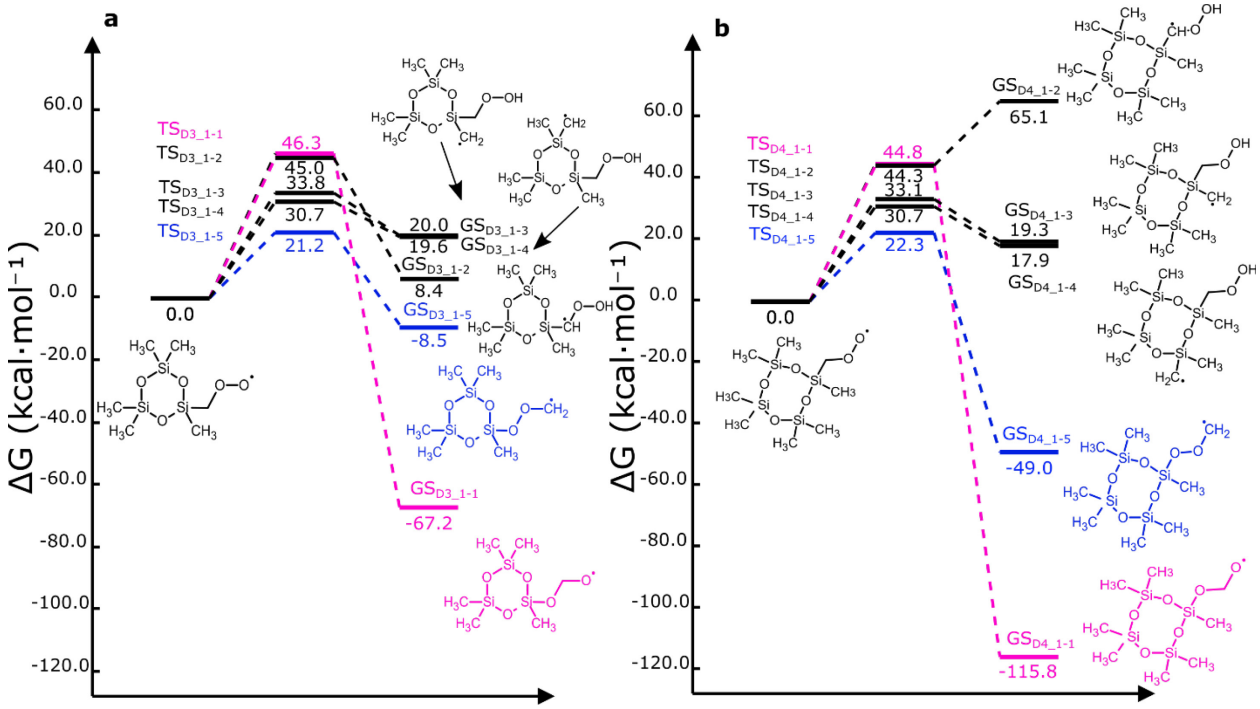

Figure 1 Potential energy surfaces of the different possible unimolecular reactions for the RO_2 from (a) D3 and (b) D4 oxidation investigated in this work. GS is ground state, and TS is transition state.

We used transition state theory (TST) at the high-pressure limit to estimate rate constants of the proposed reactions, with the results listed in Table 1. Only the results using the M06-2X level of theory with cc-pVDZ(T) basis set were used to calculate the rates. As expected from the PES for the $RO_2^{\bullet}$ reactions, only the most favorable unimolecular reaction, proceeding via TS_{1-5} will be competitive. This isomerization reaction rate constant is calculated to be 1×10^{-2} s^{-1} for the D3

derived $RO_2^•$ and 3×10^{-3} s^{-1} for the D4 derived $RO_2^•$. The rate constant for the D3 $RO_2^•$ isomerization (1×10^{-2} s^{-1}, with a ΔE of 20.3 kcal/mol) agrees with the previously reported theoretical rate of 8×10^{-3} s^{-1} (with a ΔE of 18.4 kcal/mol), suggesting consistency between the different computational methods.

3.1.2 $R_3SiO^•$ reactions

As discussed in Sect. 3.1.1, the product (GS_{1-5}) will decompose and form a siloxy radical ($R_3SiO^•$) and formaldehyde.[11] In typical carbon-based systems, the alkoxy radical analogue ($RO^•$) to the siloxy radical can decompose, react with O_2, or isomerize through intramolecular hydrogen transfer reactions. Previous computational results suggest that decomposition and reaction with O_2 are negligible for the siloxy radical,[11] and thus we neglect these pathways here.

The siloxy radical can isomerize through a hydrogen abstraction from the methyl group on a different Si atom (TS_{2-1}, ΔE of 8.7 kcal/mol and 4.9 kcal/mol for D3 and D4, respectively) or on the same Si atom as the siloxy radical (TS_{2-2}, ΔE of 24.9 kcal/mol and 24.8 kcal/mol for D3 and D4, respectively), as shown in Figure 2. The abstraction from a methyl group on the same Si atom has a significantly higher energy barrier than abstraction from the methyl group on an adjacent methyl group, as seen in Figure 2, leading to TS_{2-1} being the likely dominant isomerization pathway, which is the same anticipated pathway predicted previously.[11] These results are ~15-20% larger than previous calculations, which found D3 TS_{2-1} and TS_{2-2} have energy barriers of 7.5 kcal/mol and 20.9 kcal/mol, respectively,[11] but both methods suggest the 1,5-shift is much more favorable. Although the siloxanol functional group is formed from this isomerization, a carbon centered radical remains. Based on previous results by Fu et al.,[11] we expect that the carbon centered radical react with O_2 to form another $RO_2^•$, isomerize, and fragment releasing formaldehyde and creating a siloxy radical, allowing the radical to continue through a transition

state like $TS_{2\text{-}1}$. It is anticipated that as the number of siloxanol groups elsewhere on the ring increases so does the rate of the isomerization reaction ($TS_{1\text{-}5}$).[11] This would rapidly lead to a series of siloxanol substitutions on a single VMS molecule.

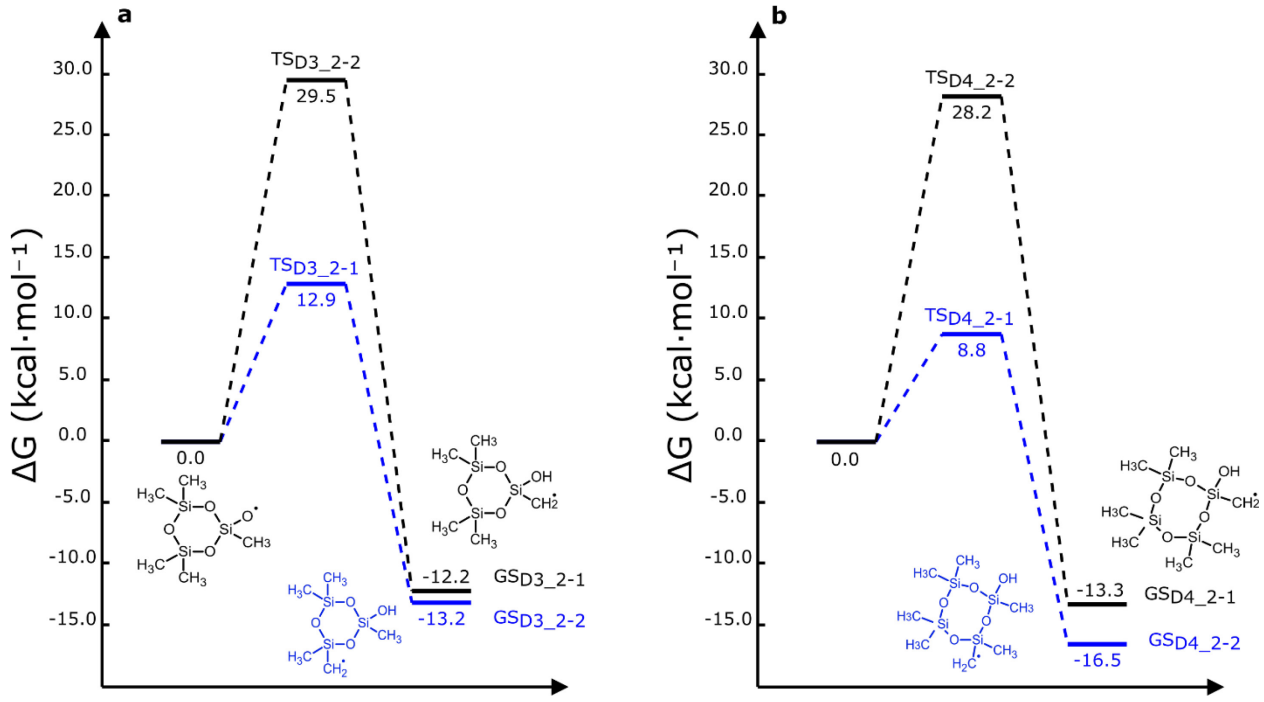

Figure 2 Potential energy surfaces for the two investigated unimolecular reactions the siloxy radical can undergo for (a) D3 and (b) D4.

We consider two new bimolecular reactions of the siloxy radical, reaction with $HO_2^{\bullet}$ and H_2O, that we previously suggested based on experimental results.[6] Although the reaction of an alkoxy radical with H_2O is not a typical gas-phase atmospheric reaction, previous studies suggest that the siloxy radical can react with water forming the siloxanol product.[26,27] Our previous work suggested that as the amount of water vapor present during D3 oxidation increases, so does the importance of the siloxanol compared to the formate ester.[6] Therefore, the siloxanol product was proposed to be formed from the bimolecular reaction of the siloxy radical with either $HO_2^{\bullet}$ or H_2O.[4,6]

Table 2 Results from theoretical calculations of $R_3SiO^{\bullet}$ reactions with the M06-2X functional optimized geometries.

Reaction	VMS	ΔG[a] (kcal/mol)	ΔE (kcal/mol)	k (s^{-1})	k (cm^3 $molec^{-1}$ s^{-1})
$R_3SiO^{\bullet}$ 1,5 H-Shift ($TS_{2\text{-}1}$)	D3	12.9	8.7	6×10^{5}	-
	D4	8.8	4.9	7×10^{8}	-
$R_3SiO^{\bullet}$ 1,3 H-Shift ($TS_{2\text{-}2}$)	D3	29.5	24.9	1×10^{-6}	-
	D4	28.2	24.8	1×10^{-5}	-
$R_3SiO^{\bullet}+H_2O \rightarrow R_3SiOH+{}^{\bullet}OH$ ($TS_{3\text{-}1}$)	D3	11.9	1.4	4×10^{2} [b]	1×10^{-15}
	D4	10.0	-1.0	1×10^{4} [b]	4×10^{-14}
$R_3SiO^{\bullet}+HO_2^{\bullet} \rightarrow R_3SiOH+O_2$ ($TS_{3\text{-}2}$)	D3	12.8	4.3	1×10^{-9} [c]	2×10^{-18}
	D4	10.8	-0.8	7×10^{-8} [c]	1×10^{-16}

[a]ΔG and ΔE reported here are corrected for zero-point vibrational energies. [b]Assuming a H_2O concentration of 3×10^{17} molec cm^{-3}, corresponding to a relative humidity of ~40% at room temperature. [c]Assuming a $HO_2^{\bullet}$ concentration of 6×10^{8} molec cm^{-3}.[28]

The PES of the two bimolecular reactions are shown in Figure 3. Although the products from the reaction with $HO_2^{\bullet}$ are significantly more stable, the reaction with H_2O has a slightly lower Gibbs free energy barrier than with the reaction with $HO_2^{\bullet}$ (Table 2). In addition, the concentration of H_2O in the atmosphere is almost always significantly higher than $HO_2^{\bullet}$, suggesting reaction with H_2O will out-compete reaction with $HO_2^{\bullet}$. Both reactions lead to the formation of the closed shell siloxanol.

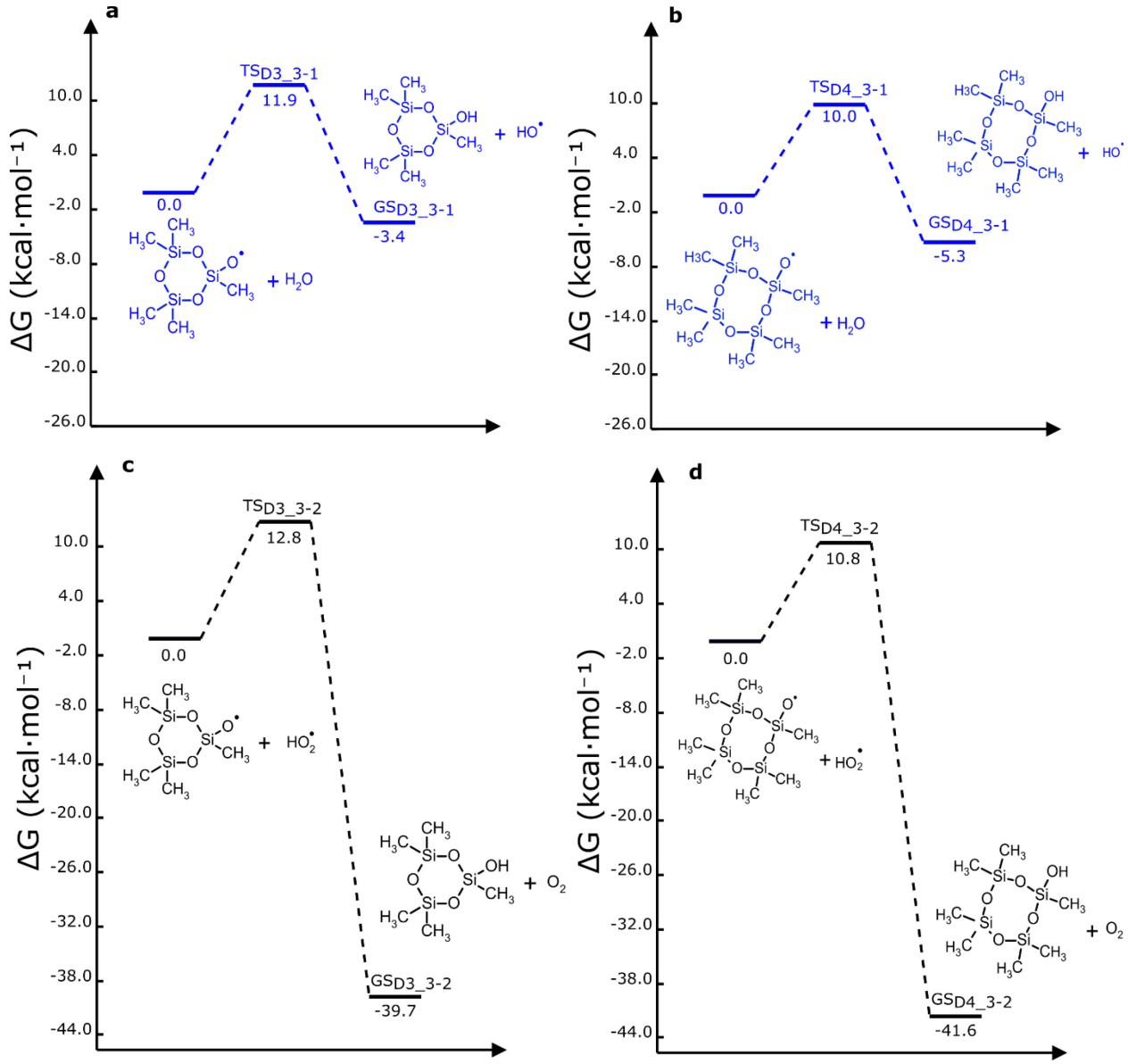

Figure 3 Potential energy surfaces for bimolecular reactions of the (a) D3 siloxy radical and (b) D4 siloxy radical with H_2O and the reaction of (c) D3 siloxy radical and (d) D4 siloxy radical with $HO_2^{\cdot}$. (a) and (b) are blue as they are anticipated to be more likely than (c) or (d).

To compare the likelihood of the $R_3SiO^{\bullet}$ undergoing isomerization reactions versus bimolecular reactions with H_2O or $HO_2^{\bullet}$, the kinetics of these reactions needs to be considered. As shown in Table 2, the unimolecular autooxidation reaction proceeding through $TS_{2\text{-}1}$ is calculated to be faster than the reaction proceeding through $TS_{2\text{-}2}$. In terms of the bimolecular reactions of the siloxy radical with H_2O and $HO_2^{\bullet}$, the reaction between the siloxy radical and H_2O for D3 and D4 is

significantly more favorable than reaction with $HO_2^{\bullet}$, as presented in Table 3. However, the rates of the bimolecular reactions are too slow to compete with the unimolecular reactions. Additionally, the calculated rate constant for $TS_{2\text{-}1}$ for D3 is $6\times10^5\ s^{-1}$, which is comparable (within a factor of 2) to a previously calculated rate of $1.1\times10^6\ s^{-1}$ for the same reaction.[11]

3.1.3 Overall fate of $R_3SiCH_2O_2^{\bullet}$ isomerization pathway

Overall, the computational results suggest that the isomerization reaction for the D3-derived $RO_2^{\bullet}$ is faster than for the D4-derived $RO_2^{\bullet}$. Additionally, the siloxy radical formed following the $RO_2^{\bullet}$ isomerization is most likely going to undergo a 1,5-hydrogen shift reaction, presumably initiating a rapid series of reactions resulting in the conversion of multiple methyl groups to hydroxyl groups. These results stand in contrast with our hypothesis that the D4-derived $RO_2^{\bullet}$ would undergo a faster isomerization ($TS_{1\text{-}5}$) than for the D3-derived $RO_2^{\bullet}$ and that the resulting siloxy radical would undergo a bimolecular reaction with H_2O or $HO_2^{\bullet}$ to form the single alcohol siloxanol. In our experimental results, we failed to detect products with more than two hydroxyl groups (instead of the six expected with rapid autoxidation for D3 or eight for D4), which could be due to wall/tubing losses, but we do not believe that is the case as there was not a significant missing fraction of product signal compared to parent loss during oxidaiton.[6] It is also possible that the experimental setup was not able to achieve long enough $RO_2^{\bullet}$ lifetimes to form the siloxanol with multiple -CH_3 to -OH conversions.

3.2 Thermodynamics and kinetics of $R_3SiCH_2O_2^{\bullet}$ reactions with $HO_2^{\bullet}$

Measurements suggest that D3 oxidation results in a larger yield of the formate ester product than D4 oxidation, which forms more of the siloxanol. As we previously hypothesized that the reaction between $RO_2^{\bullet}$ and $HO_2^{\bullet}$ ultimately leads to the formate ester,[6,11] we suggested that the reaction of $RO_2^{\bullet}$ and $HO_2^{\bullet}$ will be faster for D3 than D4 since we see higher apparent formate ester

yield with D3 than D4. Additionally, we suggested that this reaction would lead to the formation of an alkoxy radical (necessary to form the formate ester) rather than the "typical" hydroperoxide reaction product. Here we investigated the formation of the hydroperoxide and O_2 on a triplet surface and the two-step reaction of the formation of a $RO_2 \cdot HO_2$ complex followed by decomposition to $RO^{\bullet}$ and $HO_3^{\bullet}$ (which is expected to decompose to $^{\bullet}OH$ and O_2) on a singlet surface, with the energetics shown in Figure 4. We did not investigate the reaction of $RO_2^{\bullet}$ with $HO_2^{\bullet}$ to form ROH and O_3, as that has been shown to be most important for carbonyl-containing organoperoxy radicals, which are not present in our system.[29] From the calculated reaction energies, the reaction of D3-derived and D4-derived $RO_2^{\bullet}$ with $HO_2^{\bullet}$ to form the hydroperoxide is likely to outcompete the alternative reaction pathway to form the alkoxy radical due to the large ΔG barrier of the $TS_{4\text{-}2}$.

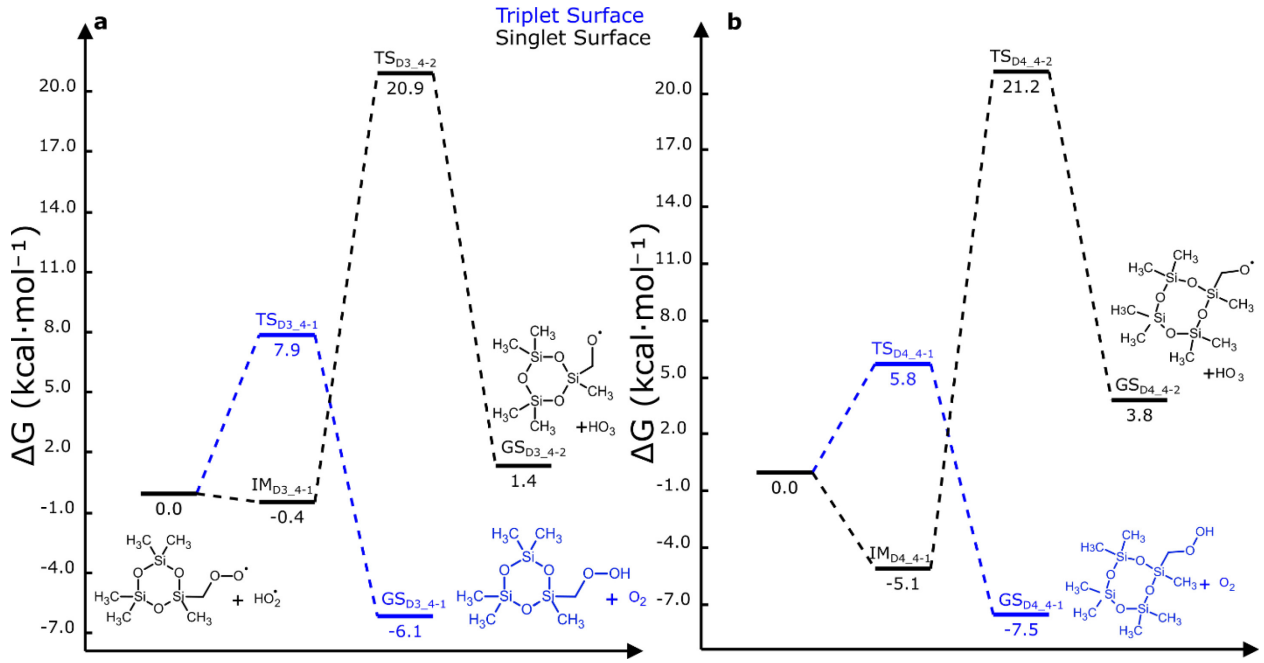

Figure 4 Potential energy surfaces for reactions of the (a) D3 and (b) D4 $RO_2^{\bullet}$ reactions with $HO_2^{\bullet}$. IM signifies intermediate.

The more favorable bimolecular reaction of $RO_2^{\bullet}$ with $HO_2^{\bullet}$ to form the hydroperoxide (ROOH) has a rate constant of 3×10^{-13} cm^3 $molec^{-1}$ s^{-1} for D3 and 2×10^{-11} cm^3 $molec^{-1}$ s^{-1} for D4. The

bimolecular rate coefficients for D3 $RO_2^\bullet$ reactions with $HO_2^\bullet$ is smaller than the "typical" assumption of ~1×10^{-11} cm^3 $molec^{-1}$ s^{-1} for these types of reactions.[30] However, the D4 $RO_2^\bullet$ reaction with $HO_2^\bullet$ is comparable to the general rate constant. Our original hypothesis (H2) was that the product of the D4-derived $RO_2^\bullet$ reaction with $HO_2^\bullet$ is the peroxy radical (to a greater extent than for the D3-derived $RO_2^\bullet$), based on experimental evidence showing the observed oxidation products of D4 were relatively independent of initial $RO_2^\bullet$ fate. This hypothesis was unsupported by the calculations. However, because the reaction between $RO_2^\bullet$ and $HO_2^\bullet$ is slower than anticipated for D3, there is the potential for alternative chemistry in a variety of atmospheric conditions which should be investigated.

Table 3 Results for bimolecular reactions of the peroxy radical with $HO_2^\bullet$

Reaction	VMS	ΔG (kcal/mol)	ΔE (kcal/mol)	k (cm^3 $molec^{-1}$ s^{-1})
$R_3SiCH_2O_2^\bullet + HO_2^\bullet \rightarrow R_3SiCH_2OOH + O_2$	D3	7.9	-5.6	3×10^{-13}
($TS_{4\text{-}1}$)	D4	5.8	-5.2	2×10^{-11}
$R_3SiCH_2O_2^\bullet + HO_2^\bullet \rightarrow R_3SiCH_2O^\bullet + HO_3^\bullet$[a]	D3	20.9	17.3	-[b]
($TS_{4\text{-}2}$)	D4	21.2	17.1	-

[a]ΔG and ΔE are calculated from the $RO_2 \cdot HO_2$ complex to the decomposition transition state ($TS_{4\text{-}2}$). [b]The rate constant is not calculated for $TS_{4\text{-}2}$ as they have significantly higher energy barriers than $TS_{4\text{-}1}$ and will not be competitive.

3.3 Comparison to experiment

Our new results suggest that reinterpretation of the experimental observations and H1/H2 may be necessary. Our previous work had assumed general rate coefficients for reactions of $RO_2^\bullet$ with $HO_2^\bullet$ of 1.7×10^{-11} cm^3 $molec^{-1}$ s^{-1},[6] a value that is two orders of magnitude faster than determined here for D3 $RO_2^\bullet$. Because of this difference in rate coefficient, the experiments for which we calculated that >90% of the $RO_2^\bullet$ reacted with $HO_2^\bullet$ in fact had only ~30% of $RO_2^\bullet$ reacting through

this pathway. This change in $RO_2^{\bullet}$ fate could explain why we detected minimal signal for the hydroperoxide product for the D3 reactions but does not explain why the hydroperoxides were not detected in the D4 experiments. One possibility is that the hydroperoxide product could be unstable and decompose, forming the alkoxy radical though an alternative, yet to be determined, pathway.

Our theoretical results cannot explain the formation of the siloxanol product in any condition. It is particularly difficult to explain in high NO conditions, where we anticipate the formate ester product should dominate. Therefore, more investigation is needed on the different reaction pathways the initial $RO_2^{\bullet}$ radical can take in high NO conditions which will likely be a previously unexplored reaction pathway.

4 Atmospheric Implications

To understand siloxane derived $RO_2^{\bullet}$ fate in a variety of atmospheric scenarios, we use data from the California Research at the Nexus of Air Quality (CalNex) campaign to represent an urban atmosphere and data from the Southern Oxidant and Aerosol Study (SOAS) to represent rural conditions. Urban conditions assumed midday mixing ratios of 10 ppt $HO_2^{\bullet}$ and 5 ppb NO.[31,32] For rural conditions, we assumed midday mixing ratios of 25 ppt $HO_2^{\bullet}$ and 50 ppt NO.[28,33] For indoor conditions, we assume an $HO_2^{\bullet}$ mixing ratio of approximately 0.8 ppt[34,35] and 2 ppt for NO.[36] Lifetimes of siloxane derived $RO_2^{\bullet}$ radicals based on these conditions are presented in Figure 5.

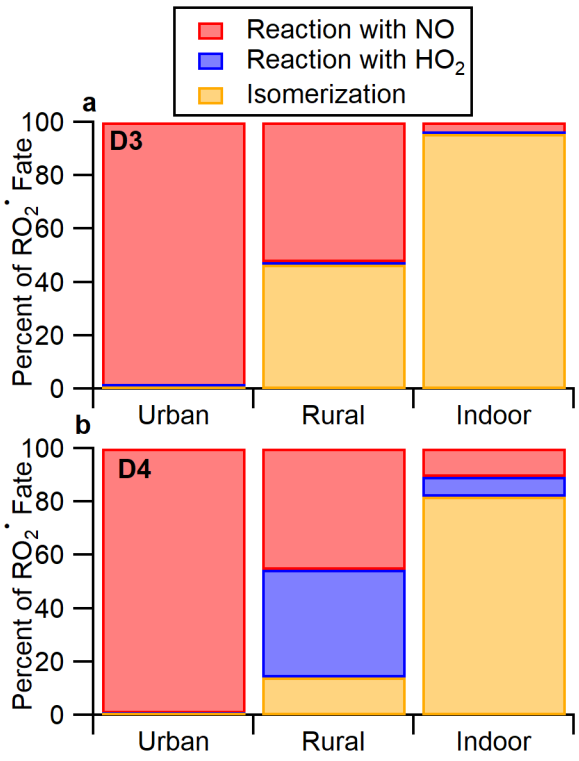

Figure 5 Bar chart showing the percent of the $RO_2^{\bullet}$ that isomerizes, reacts with $HO_2^{\bullet}$, or reacts with NO for (a) D3 and (b) D4.

Figure 5 shows the fraction of the $RO_2^{\bullet}$ reacting with NO or $HO_2^{\bullet}$ in addition to isomerizing through $TS_{1\text{-}5}$ in urban, rural, and indoor atmospheres. Reaction with NO is the dominant fate of both D3 and D4 in urban environments. Owing to the difference in the isomerization reaction rates ($TS_{1\text{-}5}$), the $RO_2^{\bullet}$ fate diverges in indoor and rural/remote conditions. As D4 and D5 have higher atmospheric concentrations than D3, reactions of D4 are likely more informative in thinking about siloxane environmental fate.[37–39] We assume that D5 will behave more similarly to D4 than to D3 and thus the main $RO_2^{\bullet}$ reactions that occur are bimolecular reactions with NO in urban environments but autoxidation in indoor environments with low NO concentrations, which is the same for D3. This is important as detrimental health effects were suggested from the release of formaldehyde during VMS autoxidation[11] in indoor environments where there are low concentrations of NO and high concentrations of D5.[40] D4 $RO_2^{\bullet}$ reactions with $HO_2^{\bullet}$ can be

important in rural conditions, whereas D3 $RO_2^{\bullet}$ will generally not react with $HO_2^{\bullet}$ due to its slower rate constant.

5. Conclusions

In this work we investigated the radical reactions occurring during the atmospheric oxidation of D3 and D4 to better understand the formation of previously observed experimental oxidation products and to reconcile the products detected experimentally with those predicted by theoretical calculations. Our original hypotheses, H1 and H2, were not supported by our calculations leaving open questions about the siloxanol product formation mechanism. However, we note that the reaction of D3 $RO_2^{\bullet}$ with $HO_2^{\bullet}$ is slower than anticipated by approximately one order of magnitude. Therefore, it was determined that the reaction with NO is likely the most important fate of the initial $RO_2^{\bullet}$. There is still uncertainty surrounding the formation of the single siloxanol product. It is particularly difficult to explain the formation of the siloxanol under conditions where $RO_2^{\bullet}$ is expected to react with NO. Based on theory, this pathway is expected to form the formate ester product rather than the siloxanol. The investigated reactions show unique chemistry that Si-containing organic molecules can undergo in the atmosphere, such as $RO_2^{\bullet}$ isomerization, decomposition reactions, and reactions with H_2O. There are also likely other unusual reactions that have yet to be identified that are key in forming the formate ester. This mostly unknown chemistry leaves room for future investigations of siloxane atmospheric oxidation.

ASSOCIATED CONTENT

Supporting Information.

The following files are available free of charge.

Supplemental information containing the coordinates of the geometries used in this work, more

information about the methods used to calculate the kinetics of these reactions, and information on sensitivity to choice of D4-derived peroxy radical conformer. (PDF)

AUTHOR INFORMATION

Corresponding Author

Eleanor C. Browne − Department of Chemistry, University of Colorado, Boulder, Colorado 80309, United States; Cooperative Institute for Research in Environmental Sciences, University of Colorado, Boulder, Colorado 80309, United States; orcid.org/0000-0002-8076-9455; Phone: 303-735-7685; Email: Eleanor.Browne@Colorado.edu

Present Addresses

[&]Now at Aerodyne Research, Incorporated. 45 Manning Road, Billerica, MA

Author Contributions

The manuscript was written by MA with guidance and feedback from EB, VJ, and SS. Conceptualization of the work was done by EB and MA. Theoretical methods were developed by MA, VJ, and SS. Calculations were performed by MA and VJ. All authors have given approval to the final version of the manuscript.

ACKNOWLEDGMENT

This work utilized the Summit supercomputer, which is supported by the National Science Foundation (awards ACI-1532235 and ACI-1532236), the University of Colorado Boulder, and Colorado State University. The Summit supercomputer is a joint effort of the University of Colorado Boulder and Colorado State University.

MA was supported in part by the Cooperative Institute for Research in Environmental Sciences Graduate Fellowship Grant and the NOAA cooperative agreement NA22OAR4320151, the Cooperative Institute for Earth System Research and Data Science. ECB and MA acknowledge support from the National Science Foundation under Grants CHE-1808606 and AGS-2029017.

VJ was supported by the National Science Foundation Graduate Research Fellowship under Grant No. DGE 2040434. SS was supported through the National Science Foundation grant CHE-2145209.

REFERENCES

(1) Organisation for economic co-operation and development. The 2004 OECD List of High Production Volume Chemicals. *Organisation for Economic Co-Operation and Development* **2004**, *C*, 66.
(2) US Environmental Protection Agency. *Comptox Dashboard*; High Production Volume List Decamethylcyclopentasiloxane. https://comptox.epa.gov/dashboard/chemical/details/DTXSID1027184 (accessed June 2023).
(3) Mackay, D.; Cowan-Ellsberry, C. E.; Powell, D. E.; Woodburn, K. B.; Xu, S.; Kozerski, G. E.; Kim, J. Decamethylcyclopentasiloxane (D5) Environmental Sources, Fate, Transport, and Routes of Exposure. *Environmental Toxicology and Chemistry* **2015**, *34* (12), 2689–2702. https://doi.org/10.1002/etc.2941.
(4) Alton, M. W.; Browne, E. C. Atmospheric Chemistry of Volatile Methyl Siloxanes: Kinetics and Products of Oxidation by OH Radicals and Cl Atoms. *Environmental Science and Technology* **2020**, *54* (10), 5992–5999. https://doi.org/10.1021/acs.est.0c01368.
(5) Atkinson, R.; Tuazon, C.; C Kwok, E. S.; Arey, J.; Aschmann, S. M.; Bridier, I. Kinetics and Products of the Gas-Phase Reactions of (CH , with CI Atoms and OH Radicals. **1995**, *91* (18), 3033–3039.
(6) Alton, M. W.; Browne, E. C. Atmospheric Degradation of Cyclic Volatile Methyl Siloxanes: Radical Chemistry and Oxidation Products. *ACS Environmental Au* **2022**, *2* (3), 263–274. https://doi.org/10.1021/acsenvironau.1c00043.
(7) Atkinson, R.; Tuazon, E. C. C.; Kwok, E. S. C. S. C.; Arey, J.; Aschmann, S. M. M.; Bridier, I. Kinetics and Products of the Gas-Phase Reactions of (CH3)4Si, (CH3)3SiCH2OH, (CH3)3SiOSi(CH3)3 and (CD3)3SiOSi(CD3)3 with Cl Atoms and OH Radicals. *Journal of the Chemical Society, Faraday Transactions* **1995**, *91* (18), 3033–3039. https://doi.org/10.1039/FT9959103033.
(8) Xiao, R.; Zammit, I.; Wei, Z.; Hu, W. P.; MacLeod, M.; Spinney, R. Kinetics and Mechanism of the Oxidation of Cyclic Methylsiloxanes by Hydroxyl Radical in the Gas Phase: An Experimental and Theoretical Study. *Environmental Science and Technology* **2015**, *49* (22), 13322–13330. https://doi.org/10.1021/acs.est.5b03744.
(9) Milani, A.; Al-Naiema, I. M.; Stone, E. A. Detection of a Secondary Organic Aerosol Tracer Derived from Personal Care Products. *Atmospheric Environment* **2021**, *246* (July), 118078. https://doi.org/10.1016/j.atmosenv.2020.118078.
(10) Atkinson, R. Gas-Phase Tropospheric Chemistry of Organic Compounds: A Review. *Atmospheric Environment* **2007**, *41* (SUPPL.), 200–240. https://doi.org/10.1016/j.atmosenv.2007.10.068.
(11) Fu, Z.; Xie, H. Bin; Elm, J.; Guo, X.; Chen, J. Formation of Low-Volatile Products and Unexpected High Formaldehyde Yield from the Atmospheric Oxidation of Methylsiloxanes. *Environmental Science and Technology* **2020**, *54* (12), 7136–7145. https://doi.org/10.1021/acs.est.0c01090.

(12) Ren, Z.; Da Silva, G. Auto-Oxidation of a Volatile Silicon Compound: A Theoretical Study of the Atmospheric Chemistry of Tetramethylsilane. *Journal of Physical Chemistry A* **2020**, *124* (32), 6544–6551. https://doi.org/10.1021/acs.jpca.0c02922.
(13) Praske, E.; Otkjær, R. V.; Crounse, J. D.; Hethcox, J. C.; Stoltz, B. M.; Kjaergaard, H. G.; Wennberg, P. O. Atmospheric Autoxidation Is Increasingly Important in Urban and Suburban North America. *Proceedings of the National Academy of Sciences of the United States of America* **2018**, *115* (1), 64–69. https://doi.org/10.1073/pnas.1715540115.
(14) Crounse, J. D.; Paulot, F.; Kjaergaard, H. G.; Wennberg, P. O. Peroxy Radical Isomerization in the Oxidation of Isoprene. *Physical Chemistry Chemical Physics* **2011**, *13* (30), 13607–13613. https://doi.org/10.1039/c1cp21330j.
(15) Crounse, J. D.; Nielsen, L. B.; Jørgensen, S.; Kjaergaard, H. G.; Wennberg, P. O. Autoxidation of Organic Compounds in the Atmosphere. *Journal of Physical Chemistry Letters* **2013**, *4* (20), 3513–3520. https://doi.org/10.1021/jz4019207.
(16) Carter, W. L. P.; J, P.; Malkina, I. L.; D, L. *Investigation of the Ozone Formation Potential of Selected Volatile Silicone Compounds; Final Report to Dow Corning Corporation*; Midland, MI, 1992.
(17) Allen, R. B.; Annelin, R. B.; Atkinson, R.; Carpenter, J. C.; Carter, W. L. P.; Chandra, G.; Fendinger, N. J.; Gerhards, R.; Grigoras, S.; Hatcher, J. A. et al. *Organosilicon Materials*; Chandra, G., Ed.; The Handbook of Environmental Chemistry; Springer Berlin Heidelberg: Berlin, Heidelberg, 1997; Vol. 3. https://doi.org/10.1007/978-3-540-68331-5.
(18) Avery, A. M.; Alton, M. W.; Canagaratna, M. R.; Krechmer, J. E.; Sueper, D. T.; Bhattacharyya, N.; Hildebrandt Ruiz, L.; Brune, W. H.; Lambe, A. T. Comparison of the Yield and Chemical Composition of Secondary Organic Aerosol Generated from the OH and Cl Oxidation of Decamethylcyclopentasiloxane. *ACS Earth Space Chem.* **2023**, *7* (1), 218–229. https://doi.org/10.1021/acsearthspacechem.2c00304.
(19) Hasson, A. S.; Tyndall, G. S.; Orlando, J. J. A Product Yield Study of the Reaction of HO 2 Radicals with Ethyl Peroxy (C 2H 5O 2), Acetyl Peroxy (CH 3C(O)O 2), and Acetonyl Peroxy (CH 3C(O)CH 2O 2) Radicals. *Journal of Physical Chemistry A* **2004**, *108* (28), 5979–5989. https://doi.org/10.1021/jp048873t.
(20) Frisch, M. J.; Trucks, G. W.; Schlegel, H. B.; Scuseria, G. E.; Robb, M. A.; Cheeseman, J. R.; Scalmani, G.; Barone, V.; Petersson, G. A.; Nakatsuji, H. et al. Gaussian 16, Revision A.03. Gaussian, Inc.: Wallingford CT 2016.
(21) Anderson, J.; Burns, P. J.; Milroy, D.; Ruprecht, P.; Hauser, T.; Siegel, H. J. Deploying RMACC Summit: An HPC Resource for the Rocky Mountain Region. In *Proceedings of PEARC17*; New Orleans, LA, 2017; p 7.
(22) Kállay, M.; Nagy, P. R.; Mester, D.; Rolik, Z.; Samu, G.; Csontos, J.; Csóka, J.; Szabó, P. B.; Gyevi-Nagy, L.; Hégely, B. et al. The MRCC Program System: Accurate Quantum Chemistry from Water to Proteins. *Journal of Chemical Physics* **2020**, *152* (7), 074107-1-18. https://doi.org/10.1063/1.5142048.
(23) Sylvetsky, N.; Banerjee, A.; Alonso, M.; Martin, J. M. L. Performance of Localized Coupled Cluster Methods in a Moderately Strong Correlation Regime: Hückel-Möbius Interconversions in Expanded Porphyrins. *Journal of Chemical Theory and Computation* **2020**, *16* (6), 3641–3653. https://doi.org/10.1021/acs.jctc.0c00297.
(24) Wigner, E. On the Quantum Correction for Thermodynamic Equilibrium. *Physical Review* **1932**, *40* (5), 749–759. https://doi.org/10.1103/PhysRev.40.749.

(25) Lii-Rosales, A.; Johnson, V. L.; Sharma, S.; Fischer, A.; Lill, T.; George, S. M. Volatile Products from Ligand Addition of P(CH3)3to NiCl2, PdCl2, and PtCl2: Pathway for Metal Thermal Atomic Layer Etching. *Journal of Physical Chemistry C* **2021**, 8287-8295. https://doi.org/10.1021/acs.jpcc.1c10690.
(26) Narayanasamy, J.; Kubicki, J. D. Mechanism of Hydroxyl Radical Generation from a Silica Surface: Molecular Orbital Calculations. *Journal of Physical Chemistry B* **2005**, *109* (46), 21796–21807. https://doi.org/10.1021/jp0543025.
(27) Ma, Y.; Jiang, B.; Moosavi-Khoonsari, E.; Andersson, S.; Opila, E. J.; Tranell, G. M. Oxidation of Liquid Silicon in Air Atmospheres Containing Water Vapor. *Industrial and Engineering Chemistry Research* **2019**, *58* (16), 6785–6795. https://doi.org/10.1021/acs.iecr.9b00313.
(28) Romer, P. S.; Duffey, K. C.; Wooldridge, P. J.; Allen, H. M.; Ayres, B. R.; Brown, S. S.; Brune, W. H.; Crounse, J. D.; De Gouw, J.; Draper, D. C. et al. The Lifetime of Nitrogen Oxides in an Isoprene-Dominated Forest. *Atmospheric Chemistry and Physics* **2016**, *16* (12), 7623–7637. https://doi.org/10.5194/acp-16-7623-2016.
(29) Hasson, A. S.; Tyndall, G. S.; Orlando, J. J.; Singh, S.; Hernandez, S. Q.; Campbell, S.; Ibarra, Y. Branching Ratios for the Reaction of Selected Carbonyl-Containing Peroxy Radicals with Hydroperoxy Radicals. *Journal of Physical Chemistry A* **2012**, *116* (24), 6264–6281. https://doi.org/10.1021/jp211799c.
(30) Ziemann, P. J.; Atkinson, R. Kinetics, Products, and Mechanisms of Secondary Organic Aerosol Formation. *Chemical Society Reviews* **2012**, *41* (19), 6582–6605. https://doi.org/10.1039/c2cs35122f.
(31) Cai, C.; Avise, J.; Kaduwela, A.; DaMassa, J.; Warneke, C.; Gilman, J. B.; Kuster, W.; Gouw, J.; Volkamer, R.; Stevens, P. et al. Simulating the Weekly Cycle of NO x -VOC-HO x -O 3 Photochemical System in the South Coast of California During CalNex-2010 Campaign. *Journal of Geophysical Research: Atmospheres* **2019**, *124* (6), 3532–3555. https://doi.org/10.1029/2018JD029859.
(32) Griffith, S. M.; Hansen, R. F.; Dusanter, S.; Michoud, V.; Gilman, J. B.; Kuster, W. C.; Veres, P. R.; Graus, M.; Gouw, J. A.; Roberts, J.; Young, C. et al. Measurements of Hydroxyl and Hydroperoxy Radicals during CalNex-LA: Model Comparisons and Radical Budgets. *J. Geophys. Res. Atmos.* **2016**, *121* (8), 4211–4232. https://doi.org/10.1002/2015JD024358.
(33) Martinez, M. OH and HO $_2$ Concentrations, Sources, and Loss Rates during the Southern Oxidants Study in Nashville, Tennessee, Summer 1999. *J. Geophys. Res.* **2003**, *108* (D19), 4617. https://doi.org/10.1029/2003JD003551.
(34) Carslaw, N.; Fletcher, L.; Heard, D.; Ingham, T.; Walker, H. Significant OH Production under Surface Cleaning and Air Cleaning Conditions: Impact on Indoor Air Quality. *Indoor Air* **2017**, *27* (6), 1091–1100. https://doi.org/10.1111/ina.12394.
(35) Kruza, M.; Shaw, D.; Shaw, J.; Carslaw, N. Towards Improved Models for Indoor Air Chemistry: A Monte Carlo Simulation Study. *Atmospheric Environment* **2021**, *262*, 118625. https://doi.org/10.1016/j.atmosenv.2021.118625.
(36) Mendez, M.; Amedro, D.; Blond, N.; Hauglustaine, D. A.; Blondeau, P.; Afif, C.; Fittschen, C.; Schoemaecker, C. Identification of the Major HOx Radical Pathways in an Indoor Air Environment. *Indoor Air* **2017**, *27* (2), 434–442. https://doi.org/10.1111/ina.12316.
(37) Genualdi, S.; Harner, T.; Cheng, Y.; MacLeod, M.; Hansen, K. M.; Van Egmond, R.; Shoeib, M.; Lee, S. C. Global Distribution of Linear and Cyclic Volatile Methyl Siloxanes

in Air. *Environmental Science and Technology* **2011**, *45* (8), 3349–3354. https://doi.org/10.1021/es200301j.
(38) Buser, A. M.; Kierkegaard, A.; Bogdal, C.; Macleod, M.; Scheringer, M.; Hungerbühler, K. Concentrations in Ambient Air and Emissions of Cyclic Volatile Methylsiloxanes in Zurich, Switzerland. *Environmental Science and Technology* **2013**, *47* (13), 7045–7051. https://doi.org/10.1021/es3046586.
(39) Gallego, E.; Perales, J. F.; Roca, F. J.; Guardino, X.; Gadea, E. Volatile Methyl Siloxanes (VMS) Concentrations in Outdoor Air of Several Catalan Urban Areas. *Atmospheric Environment* **2017**, *155*, 108–118. https://doi.org/10.1016/j.atmosenv.2017.02.013.
(40) Tang, X.; Misztal, P. K.; Nazaroff, W. W.; Goldstein, A. H. Siloxanes Are the Most Abundant Volatile Organic Compound Emitted from Engineering Students in a Classroom. *Environmental Science and Technology Letters* **2015**, *2* (11), 303–307. https://doi.org/10.1021/acs.estlett.5b00256.

TOC Graphic